Volume 14
Number 2
20 January 2026
Pages 297-602

Biomaterials Science

rsc.li/biomaterials-science

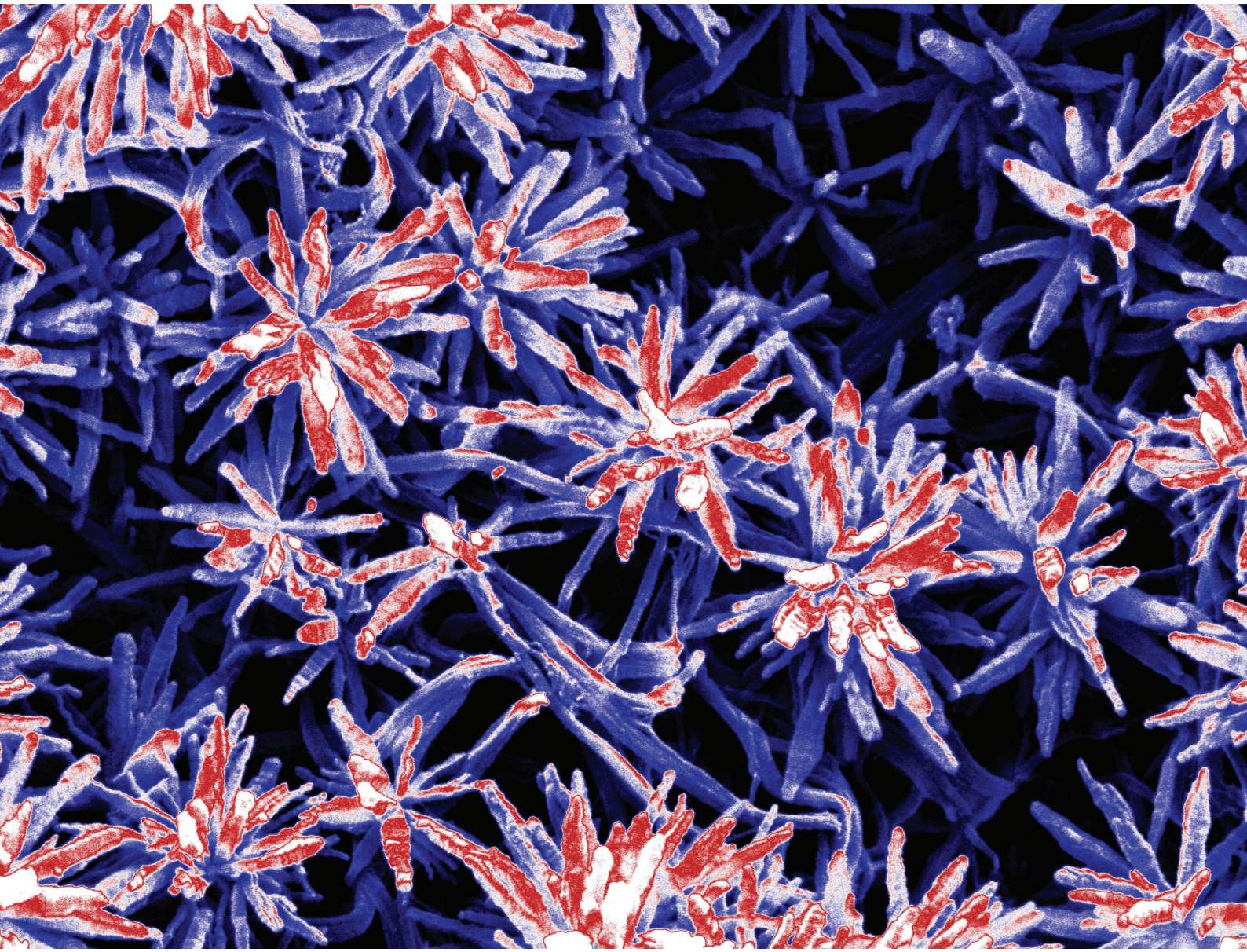

ISSN 2047-4849

ROYAL SOCIETY OF CHEMISTRY

PAPER

Hanna Solomon, Jay M. Patel *et al.*
The evaluation of platelet lysate incorporation into the microfracture clot in a pig model

ESB European Society for Biomaterials

Biomaterials Science

ROYAL SOCIETY OF CHEMISTRY

PAPER

View Article Online
View Journal | View Issue

Cite this: *Biomater. Sci.*, 2026, **14**, 440

The evaluation of platelet lysate incorporation into the microfracture clot in a pig model

Hanna Solomon,[a,b] Julie Gordon,[c] Maddie Hasson,[a,b] Hannah Arnade,[c] Jordan Parker,[c] Beatriz Dias,[c] Amogh Magesh,[a] William X. Patton,[a,b] John F. Peroni[c] and Jay M. Patel *[a,b]

Cartilage injuries present a significant clinical burden due to the tissue's limited regenerative capacity. Microfracture (Mfx) remains the gold standard of cartilage repair but often results in inadequate defect fill and inferior tissue formation. Point-of-care augmentations to the Mfx environment represent implementable and cost-effective methods to enhance outcomes. The objective of this study was to evaluate platelet lysate (PL) as an adjuvant to microfracture-based cartilage repair, with the goal of maintaining tissue volume and promoting functional repair. The impact of PL on the activity of marrow-derived cells (MDCs) was first evaluated in monolayer culture, which demonstrated an increase in cellular area and proliferation. Next, PL was incorporated into fibrin gels (to mimic fibrin-rich Mfx), and MDCs encapsulated within PL-containing fibrin gels exhibited increased proliferation, increased cellular area, and reduced fibrosis markers. PL incorporation into fibrin gels led to clear changes to initial nanostructure and an increase in initial mechanical properties, which resulted in less MDC-mediated contraction during culture. These findings suggested that time-zero augmentation of Mfx with PL may alter both cellular signaling and Mfx clot structure/remodeling. Finally, PL-augmented Mfx was evaluated in a pig trochlear osteochondral defect model (t = 5 weeks). While PL-treated defects exhibited reduced contraction and improved macroscopic appearance over Mfx alone, micro-CT and mechanical testing revealed no significant differences in subchondral bone remodeling or repair tissue stiffness. Histological analysis and grading showed no significant improvements in cartilage repair quality across treatment groups, suggesting that while PL may influence early clot stability, its effects on long-term tissue maturation remain uncertain. "Future studies are needed to determine whether PL-based augmentation provides sustained functional benefits, potentially in combination with additional biological or mechanical strategies".

Received 7th March 2025,
Accepted 8th October 2025

DOI: 10.1039/d5bm00372e

rsc.li/biomaterials-science

Introduction

Articular cartilage injuries are a prevalent and challenging issue in orthopaedic medicine, particularly due to cartilage's limited self-regenerative capabilities.[1] Cartilage lines the ends of bones in our joints and plays a critical role in reducing friction and absorbing shock during movement.[2] However, when damaged by trauma, it lacks the ability to heal effectively, often leading to progressive degeneration.[3] Over time, untreated cartilage damage can progress to osteoarthritis (OA), a debilitating condition that affects hundreds of millions globally.[4]

Among the various treatment options for articular cartilage injuries, microfracture (Mfx) remains the gold standard surgical technique for tissue repair.[5] Microfracture involves creating small holes in the subchondral bone beneath the cartilage defect to enable bone marrow elements, including marrow cells,[6] to migrate to the site of injury.[7] The marrow elements form a provisional clot, which acts as a scaffold for new tissue growth.[7,8] While Mfx can reduce pain and improve joint function in the short term, long-term results are often suboptimal.[8] The tissue that forms in the defect is typically fibrous cartilage (fibrocartilage), which lacks the mechanical properties of healthy hyaline cartilage.[9] This fibrous tissue is less durable, less elastic, and more prone to wear, potentially leading to recurrent joint problems and, eventually, OA. Additionally, the extent of defect fill following Mfx has been shown to correlate with clinical outcomes, with incomplete fill associated with poorer functional recovery and an increased risk of OA progression.[10]

Researchers have explored various strategies to enhance the effectiveness of microfracture by incorporating bioactive molecules, scaffolds, and cell-based therapies into the clot to promote better tissue quality.[11] Growth factors, like transform-

[a]*Department of Orthopaedics, Emory University School of Medicine, Atlanta, GA, USA. E-mail: jay.milan.patel@emory.edu*
[b]*Atlanta VA Medical Center, Decatur, GA, USA*
[c]*Department of Large Animal Medicine, College of Veterinary Medicine, University of Georgia, Athens, GA, USA*

ing growth factor-beta (TGF-β), insulin-like growth factor (IGF), and bone morphogenetic proteins (BMPs), have received significant attention due to their potential to modulate cell behavior and guide chondrogenesis or cartilage regeneration.[12] Despite the promise of growth factors in improving cartilage repair, translating these findings into clinical practice has proven difficult due to the complexity of cartilage regeneration and regulatory hurdles.[13–16]

Point-of-care solutions, such as autologous blood products like platelet-rich plasma (PRP), have been increasingly utilized to enhance cartilage repair.[17] PRP, which contains a concentrated amount of platelets and their associated growth factors including platelet-derived growth factor (PDGF), transforming growth factor-beta (TGF-β), and vascular endothelial growth factor (VEGF), are thought to stimulate the healing process at the injury site.[18,19] This approach is appealing due to its minimally invasive nature, low regulatory barrier, and delivery of a high concentration of regenerative factors at the repair site.[17,20] However, while this method has shown promise in enhancing tissue repair, it has yet to consistently improve repair fill and quality of tissue in clinical settings.[17,20] One potential limitation of PRP is the lack of standardization in its preparation and composition, leading to variability in platelet concentration, leukocyte content, and bioactive factor release.[21,22] This inconsistency can result in unpredictable biological effects, complicating its clinical application and limiting its widespread adoption as a reliable adjunct for cartilage repair.[21,22]

To address these limitations, the capacity of platelet lysate (PL) to enhance tissue volume maintenance and promote functional chondrogenesis in Mfx environments was examined. PL is derived from platelets and contains a rich concentration of growth factors, similar to PRP, but in a more refined form.[23] It offers a promising alternative by providing a controlled and characterized amount of growth factors through standardized platelet processing methods, such as freeze–thaw cycles.[24,25] PL also contains a higher concentration of growth factors compared to other blood-derived products. Unlike PRP, which is temperature-sensitive and cannot be stored below 4 °C, PL can be preserved at lower temperatures for extended periods, making it more stable and practical for clinical applications.[26] Prior studies have shown that PL can stimulate proliferation of mesenchymal stromal cells (MSCs), which is critical for tissue regeneration.[27] Additionally, PL has been reported to support chondrogenic differentiation *in vitro*, suggesting a potential role in promoting cartilage-like tissue formation.[28] PL also retains clotting factors, including fibrinogen, which may enhance early clot stability and the structural integrity of the repair tissue.[29] A further advantage of PL as a biologic adjunct is its feasibility for allogeneic use.[30] In contrast to autologous blood-derived products, PL can be manufactured from donor sources, standardized, and stored for clinical application making it a practical and scalable option for cartilage repair.[31]

PL provides a concentrated source of growth factors that may influence both cellular signaling and the physical properties of a microfracture (Mfx) clot.[32] While PL has been shown to promote proliferation and paracrine activity *in vitro*, its potential to alter clot stability, structure, and subsequent remodeling *in vivo* remains poorly defined. Importantly, despite extensive use of PL in musculoskeletal applications, there is limited evidence evaluating its efficacy as an adjuvant to Mfx in large animal models of chondral repair. The present study is the first to assess time-zero augmentation of Mfx with PL in a translational large animal setting, addressing a critical gap in the field.

The goal of this study was to evaluate the impact of PL on Mfx healing, both *in vitro* and *in vivo*. Two different platelet lysate formulations were investigated *in vivo*—fibrinogen-competent PL and fibrinogen-depleted PL—to determine whether the clot-promoting effects observed were primarily driven by fibrinogen content or by the growth factors present in PL. "We hypothesized that PL, through its growth factor content and fibrinogen-mediated effects, would stabilize the Mfx clot and reduce fibrocartilage formation". These findings would motivate clinical use of cost-effective and point-of-care Mfx augmentations that promote long-term volumetric and functional cartilage repair.

Experimental

Culture of hMDCs

Human bone marrow was anonymously and commercially obtained from Lonza (27-year-old male, 23-year-old male, and 36-year-old female; under approved protocols) and processed using a Ficoll gradient to isolate mononuclear cells. These donors were labeled Donors 1, 2, and 3, respectively. These cells were then plated and cultured in alpha-modified Eagle's medium (α-MEM) supplemented with 10% v/v fetal bovine serum (FBS), 1% v/v penicillin–streptomycin–fungizone (PSF), and 5 ng mL^{-1} fibroblast growth factor-2 (FGF-2) for one week. Following this initial culture period, adherent human marrow-derived stromal cells (hMDCs) were expanded, passaged, cryopreserved in a solution of 95% FBS and 5% dimethyl sulfoxide (DMSO), and stored in liquid nitrogen. hMDCs were utilized for all *in vitro* experiments at Passages 2 or 3.

Monolayer proliferation assays

A total of 50 000 hMDCs (Lonza 27-year-old male) were plated per well in a treated 24-well plate and subject to the following conditions: Dulbecco's modified Eagle's medium (DMEM) with 1% PSF (Ctl), Ctl + 10% FBS, Ctl + 2% PL, and Ctl + 10% PL. Human platelet lysate was obtained from Stem Cell Technologies (catalog #06961), a growth factor-rich supplement derived from healthy donor platelets collected at FDA-licensed blood centers. This PL was utilized for all *in vitro* experiments. All conditions were supplemented with 1 ng mL^{-1} of TGF-β3, and cells were cultured for 3 days. An MTT assay was performed using OZ Biosciences MTT Cell Proliferation Kit to assess the impact of platelet lysate on the proliferation of hMDCs. Additionally, hMDCs were seeded onto an 8-well chamber slide using the same treatments and

subsequently stained for Ki-67 to assess cell proliferation (staining protocol provided below). Four images per group were quantified for proportion of proliferative cells. This was obtained by dividing the number of Ki-67 positive cells by the number of total nuclei.

Fibrin gel nanostructure

Fibrin gel nanoarchitecture was visualized using scanning electron microscopy (SEM) to assess fibrin network organization and morphology. Fibrin gels were prepared with final concentrations of fibrinogen (25 mg mL^{-1}), thrombin (5 U mL^{-1}), calcium chloride (20 mM), with or without platelet lysate at 20% of the total volume. Samples were then fixed in glutaraldehyde (2.5% v/v) in phosphate-buffered saline (PBS) at 4 °C for 24 hours to preserve structural integrity. Following fixation, gels were dehydrated through a graded ethanol series (30%, 50%, 70%, 90%, and 100%) and then subjected to critical point drying to prevent structural collapse. Once dried, samples were coated with a thin layer of gold using a sputter coater to enhance conductivity. Imaging was performed using a field-emission SEM, capturing high-resolution images of fibrin fiber diameter, density, and overall network structure (Robert P. Apkarian Integrated Electron Microscopy Core, Emory University). Fibrin fiber diameter was quantified using ImageJ by measuring fibers from high-magnification SEM images, ensuring accurate assessment of structural differences between conditions.

Fibrin gel mechanical testing

Fibrin gel mechanical properties were evaluated using a Biomomentum Mach-1 mechanical testing system to assess their resistance to compression. Fibrin gels were prepared with final concentrations of fibrinogen (25 mg mL^{-1}), thrombin (5 U mL^{-1}), calcium chloride (20 mM), with or without platelet lysate at 20% of the total volume. Samples were submerged in phosphate-buffered saline (PBS) at 37 °C to maintain physiological conditions during testing. Unconfined compression tests were conducted using a flat, non-porous platen. A strain of ~20% was applied, following by a 120 second hold. Equilibrium modulus was quantified from the resulting load and deformation at the end of stress relaxation.

MDC response in PL-fibrin microgels

To gain a deeper understanding of how PL influences MDCs within fibrin gels, gels were prepared with final concentrations of fibrinogen (25 mg mL^{-1}), thrombin (5 U mL^{-1}), calcium chloride (20 mM), and hMDCs (200 000 cells per mL), with or without platelet lysate at 20% of the total volume. This mixture was plated in 8-well chamber slides (10 μL per well) and allowed to gel for 60 minutes. The resulting microgels were cultured for 3 days in basal media (BM; 10% FBS, 1% PSF) containing aprotinin (100 KIU per mL) and TGF-β3 (1 ng mL^{-1}). Following culture, gels were fixed and stained with Phalloidin (Cell Signaling, Catalog #8940S), Ki-67 (Thermo Fisher, Catalog #MA5-14520), SOX-9 (Thermo Fisher, Catalog #PIPA581966), and alpha smooth muscle actin (α-SMA; Sigma-Aldrich, Catalog #A2547) antibodies. For staining, fibrin gels were fixed in 10% Carson's buffered formalin for 20–30 minutes, permeabilized with 1% Triton (v/v) for 15 minutes, and blocked with 3% w/v bovine serum albumin (BSA) in PBS for 60 minutes. Primary antibody incubation was performed overnight at 4 °C in 1% w/v BSA. After a 60 minute incubation with secondary antibody and/or Phalloidin at room temperature, DAPI (1 : 100 concentration) was applied for nuclear staining for 10 minutes, and samples were mounted with Prolong Gold. Slides were imaged using confocal microscopy (Nikon A1R) to obtain *z*-stack images. Cell morphology and protein immunofluorescence were analyzed using CellProfiler. Cell boundaries were identified using thresholding algorithms, and form factor (measure of cell circularity) was computed to assess morphological changes. Microgel experiments were performed with cells from all three donors.

For Ki-67 analysis, PL was added to both the gels and/or media. Ki-67 expression was quantified as a percent of cells with positive staining, as above for monolayer cultures. For SOX-9 and α-SMA expression, maximum intensity projections were generated from confocal *z*-stacks. Fluorescence intensity was then quantified per cell to compare expression levels across experimental conditions.

Macroscale contraction during culture

hMDCs (2 million cells per mL) were incorporated into the fibrin gels (25 mg mL^{-1} fibrinogen, 5 U mL^{-1} thrombin, 20 mM $CaCl_2$) and cultured for 14 days in BM supplemented with aprotinin (100 KIU per mL) and TGF-β3 (1 ng mL^{-1}). At the end of the culture period, gel area was quantified using scanner images (600 dpi) in Image J software.

In vivo pig model

Surgical procedure. All animal procedures described in this study were approved with the Guidelines for Care by the University of Georgia Institutional Animal Care and Use Committee. Four 10 week old, female Yorkshire cross pigs weighing approximately 70 lbs, were used for this study, though one animal expired during the procedure, leaving three animals for this study. Under general anesthesia, both knees were shaved, cleaned, and surgically draped. *Via* a medial patellar arthrotomy, a lateral dislocation of the patella was used to expose the articular surface of the medial trochlea of the distal femur. In both knees, three cylindrical osteochondral defects (6 mm-diameter × ~3 mm deep) were created on the medial trochlear ridge of each animal. Defects were standardized in size and depth using a surgical punch. Following defect creation, a micropicking device was used to introduce three subchondral holes to enable marrow access. Each defect was randomized into one of three treatment groups:

1. Microfracture only (no additional treatment; Mfx).
2. Microfracture + fibrinogen-competent PL (Fib-comp PL).
3. Microfracture + fibrinogen-depleted PL (Fib-dep PL).

Allogenic pig platelet lysate was obtained from the same pig species *via* plateletpheresis. Resulting platelet concentrates were subjected to two freeze–thaw cycles to lyse the platelets

and the resulting lysate then underwent three centrifugation and filtration cycles. The resulting fibrinogen competent PL product was pooled and stored at −80 °C in 50 mL aliquots. To obtain fibrinogen depleted PL, 20 mM $CaCl_2$ was added to thawed aliquots of pooled PL, together with 0.5 g mL^{-1} 3 mm diameter glass beads (Millipore, Darmstadt, Germany), and incubated at room temperature for 30–60 minutes until a clot formed. Tubes were shaken vigorously to break up the clot, then centrifuged at 4000*g* for 30 minutes. The liquid portion (now fibrinogen-depleted) was removed using a P1000 pipet, filtered through a 40 μm nylon cell strainer (Corning, Inc), aliquoted, and stored at −80 °C.

Due to the impacts on clotting and structure observed *in vitro*, both of these formulations were tested *in vivo*. The patella was then relocated, and the joint capsule, fascia, and skin were closed in anatomical layers. Postoperative analgesics, antibiotics, and anti-inflammatories were administered according to veterinary guidelines, and the animals were returned to unrestricted cage activity once fully recovered from anesthesia. All animals were euthanized at 5 weeks post-surgery to assess early defect healing and tissue remodeling. Gross examination and subsequent analyses (*e.g.*, mechanics, micro-computed tomography [μCT], histology) were performed to evaluate the efficacy of PL supplementation in preserving defect volume and supporting Mfx cartilage repair.

Biomechanical mapping. After the animals were euthanized, each knee joint was carefully dissected to expose and isolate each osteochondral defect. Macroscopic photographs were then taken to document the overall appearance of the repair tissue. Osteochondral blocks containing each defect – proximal, central, and distal – were extracted. Mechanical indentation testing was performed using a Biomomentum Mach-1 multi-axis mechanical mapping system. Indentations were conducted across the three defect regions, the cartilage neighboring the defect, and the distant healthy cartilage to evaluate how the repair tissue is maturing. Indentations consisted of a

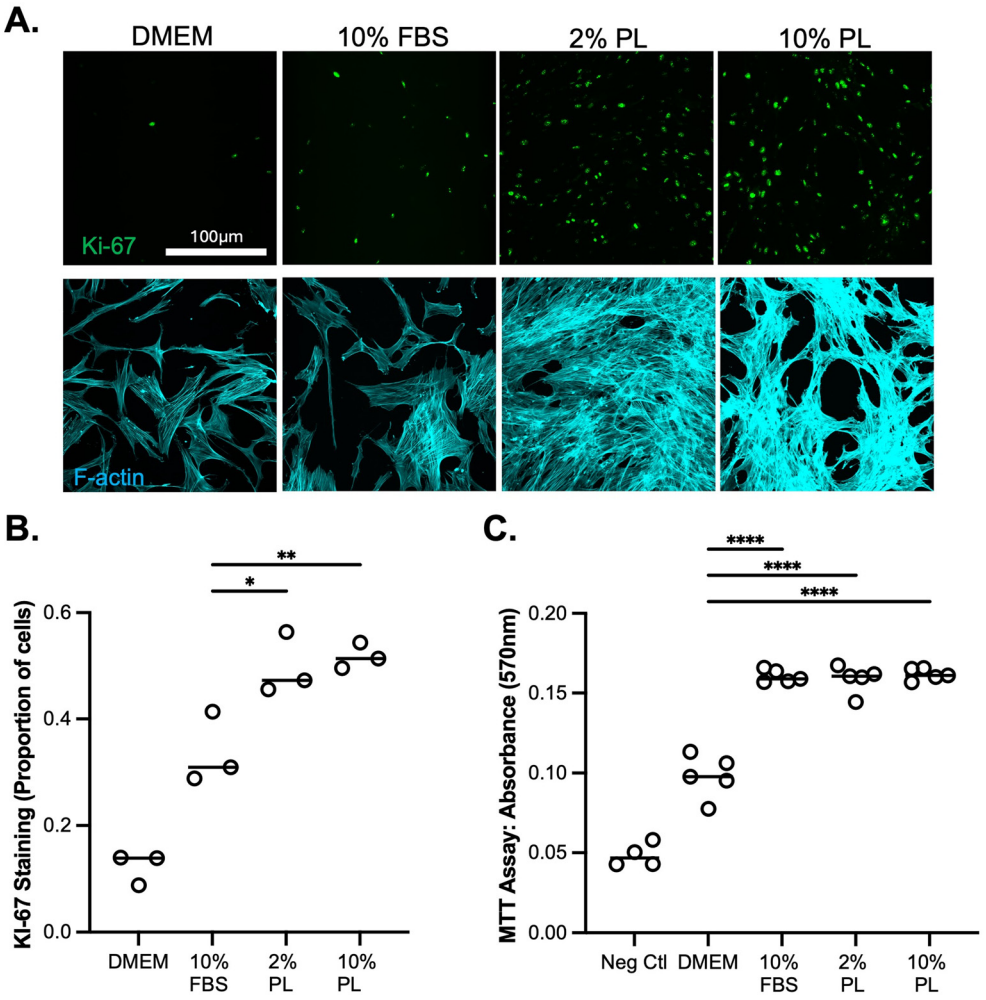

Fig. 1 [A] Ki-67 and Phalloidin staining of MDCs cultured for 3 days in monolayer with DMEM, basal media (10% FBS), 2% platelet lysate, and 10% platelet lysate. Scale bar = 100 μm. [B] Quantification of Ki-67 staining, with each plot representing 30–200 cells per image. $n = 3$ images per group. DMEM significantly lower than other three groups ($p < 0.0001$). [C] MDCs were cultured for 3 days in a 24-well treated plate for MTT assay, and absorbance was quantified. Negative controls are wells without cells. $n = 5$ per group. *$p < 0.05$, **$p < 0.01$, ****$p < 0.0001$.

find-surface, loading to 0.1 mm of indentation, and a 30 second stress relaxation hold. The resulting load-displacement data were processed and analyzed in MATLAB using a custom-designed script, which enabled quantitative assessment (instantaneous modulus, equilibrium modulus) of both repair tissue and neighboring cartilage. Samples were then fixed with formalin for one week, followed by micro-CT analysis.

μCT for defect fill and subchondral bone health. The fixed osteochondral samples were gently cleaned of excess soft tissue and placed in a scanning chamber containing phosphate-buffered saline (PBS)-soaked gauze to maintain sample hydration throughout the scanning process. Samples were scanned using a μCT system (*e.g.*, SCANCO μCT50), and the subchondral region below the defect was contoured and analyzed for structural changes (bone volume/total volume [BV/TV]), providing insights into how PL treatment influenced bone remodeling. Additionally, defect fill was quantified to assess the volume of tissue regeneration within the defect areas.

Histology for tissue quality. Following μCT, samples were decalcified for four weeks (DeCal Stat), with the solution refreshed weekly. Decalcified tissues were transferred to 70% ethanol, processed through graded ethanol dehydration and xylene clearing, and infiltrated with and embedded in hot paraffin wax. Paraffin blocks were sectioned at 5 μm thickness with sections taken from the central region of each circular defect. Safranin O/Fast Green (SafO/FG) staining was employed to evaluate tissue repair and integration. All stained slides were digitized using an automated light microscope (Olympus BX43). For semi-quantitative analyses, histological scoring was performed in accordance with the ICRS II histological grading system by three independent observers, facilitating objective comparisons between treatment groups. A modified system was used that did not assess tissue morphology (13 of 14 ICRS II outcome metrics used).

Statistical analysis. All statistical analyses were performed using GraphPad Prism which provides built-in statistical testing. For comparisons between two groups, an unpaired two-tailed *t*-test was used to assess statistical significance. For experiments involving three or more groups, a one-way analysis of variance (ANOVA) with *post hoc* Tukey's testing was conducted. Significance levels are indicated by: $*p < 0.05$; $**p < 0.01$, $***p < 0.001$, $****p < 0.0001$. All *in vitro* data within the main body manuscript are from Donor 1, and select experiments from Donors 2 and 3 are presented in the SI figures.

Results

Early cell behavior and proliferation

PL supplementation promoted a greater proportion of proliferating cells, as evidenced by Ki-67 staining (Fig. 1A). Quantification of Ki-67 positive cells confirmed a significant increase in cell proliferation in the PL-treated groups compared to controls (Fig. 1B). Further validation using an MTT assay demonstrated that proliferation rates remained consistent among conditions cultured with 10% fetal bovine serum (FBS), 2% PL, and 10% PL (Fig. 1C), showing that even a low PL concentration in the media can provide robust improvements in cellular proliferation.

Structural characterization and gel mechanics

SEM imaging revealed that PL-containing fibrin gels displayed "flower-like" microstructures on the surface, with significantly

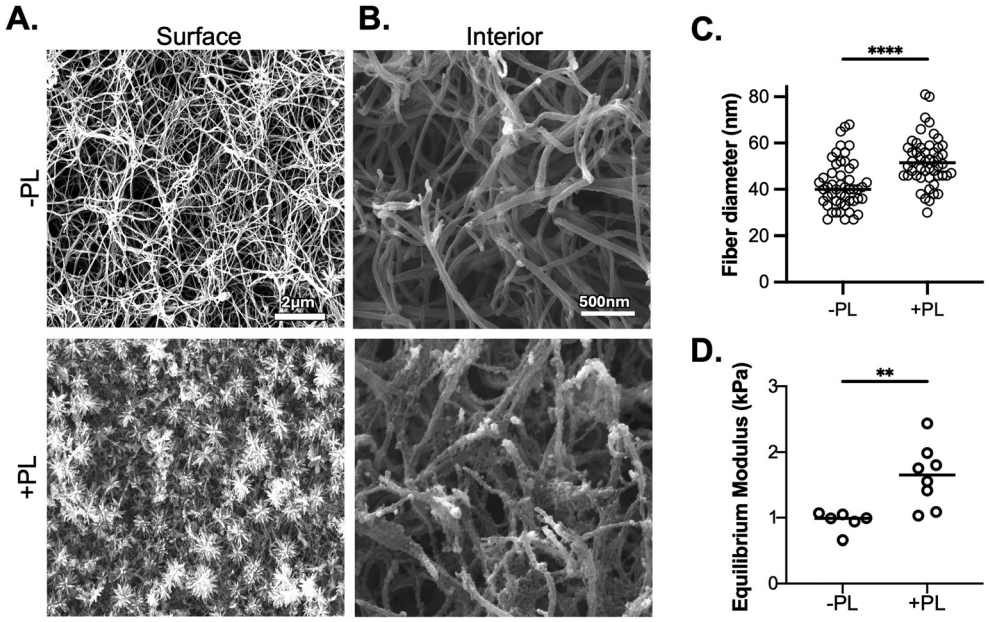

Fig. 2 Scanning electron micrographs of fibrin gels without or with platelet lysate (PL) obtained [A] on the surface or [B] within gels. Scale bar = 2 μm and 500 nm, respectively. [C] Quantification of fibrin fiber diameter within the interior of the gel. $n > 40$ fibers per group from 3 images. [D] Equilibrium modulus of fibrin gels without or with PL augmentation. $n = 6–8$ per group. $**p < 0.01$, $****p < 0.0001$.

larger fibrin fibers within the gel compared to control gels (Fig. 2A–C). Fibrin supplemented with PL also contained interior fibers that appeared rougher (less smooth) than those in their fibrin only counterparts. Mechanical testing of these gels showed that PL supplementation also significantly increased gel stiffness compared to control fibrin-only gels (Fig. 2D), suggesting that PL enhances the structural integrity of fibrin matrices.

Cell proliferation in fibrin gels

MDCs encapsulated in PL-containing fibrin gels exhibited increased proliferation in media containing both DMEM and 10% FBS, as evidenced by Ki-67 staining (Fig. 3A and B). Proliferation was further enhanced in PL gels cultured in PL media, showing even higher Ki-67 expression, which indicates a synergistic effect of both PL in the gel and PL in the culture medium. Additionally, MDCs in PL-treated gels displayed a larger, rounder morphology compared to controls (Fig. 3C). We also validated these results in two additional donors (Fig. S1) but rather than looking at different serum formulations, we looked at Ctl ± TGF-β3 and PL ± TGF-β3. These results further show how PL incorporation into gels improves Ki-67 staining across donors and across media formulations.

Cell phenotypic shifts and morphological changes

MDCs in PL-containing fibrin gels were larger and less spindly than controls, as shown by F-actin staining (Fig. 4A). Quantification revealed significantly larger cell areas (Fig. 4B) and a reduced form factor (Fig. 4C) for MDCs in PL gels. SOX-9 and α-SMA intensities were both significantly lower in PL gels (Fig. 4D and E), suggesting lower chondrogenic potential, but lower fibrotic potential as well. These results were validated in two additional donors (Fig. S2), although the reduction in form factor was less pronounced in these donors.

Macrogel contraction

PL-supplemented fibrin gels exhibited reduced contraction at the macro-scale, as evidenced by clearly larger gels compared to control gels over the culture period (Fig. 5A). Quantification of gel area at 14 days verified PL-containing gel areas (29.71 ± 6.99 mm^2) were significantly greater (79.4%; p = 0.0106) than fibrin gel counterparts (16.56 ± 1.64 mm^2). This reduction in

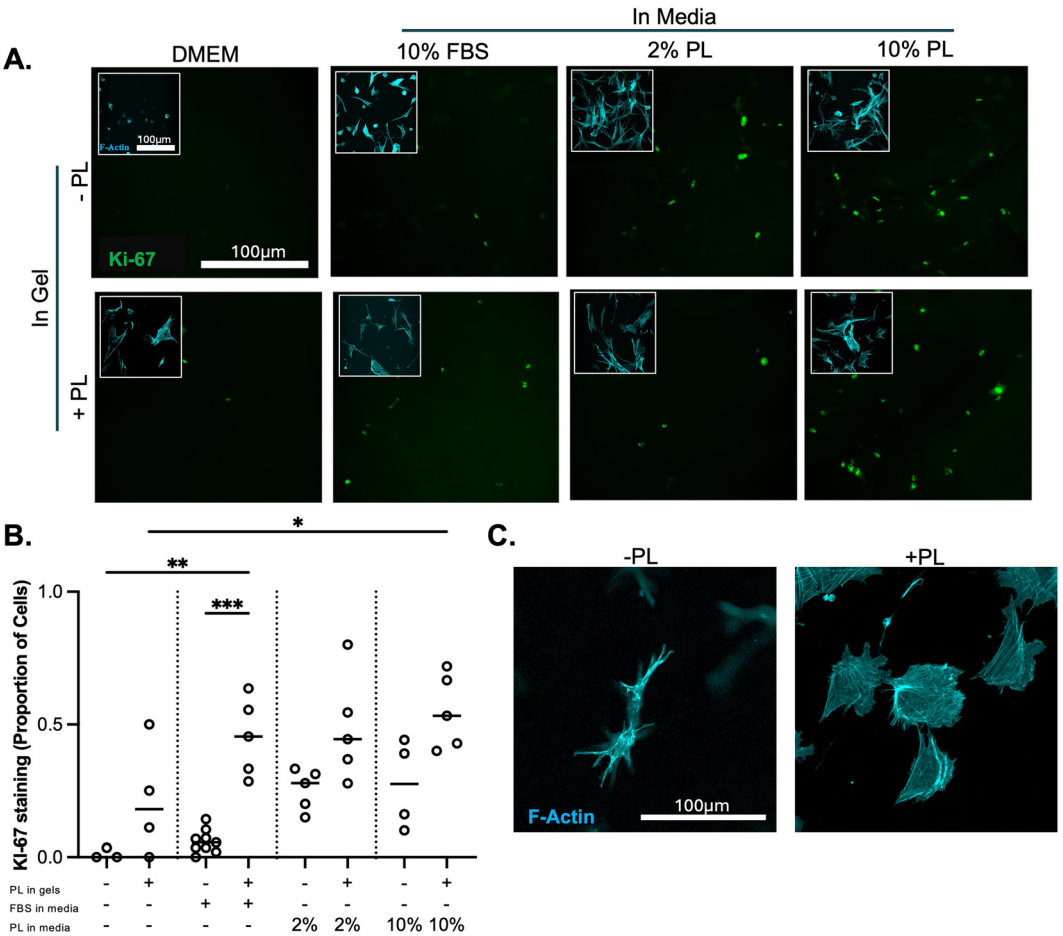

Fig. 3 [A] Ki-67 staining of MDCs cultured for 3 days in fibrin gels without or with PL, cultured in varying medias. Inset shows F-actin staining. Scale bar = 100 μm. [B] Quantification of Ki-67 staining as proportion of cells. Each plot represents 20–50 cells per image, n = 3–9 images per group. [C] F-actin staining of MDCs cultured for 3 days in fibrin gels without or with platelet lysate. Scale bar = 100 μm. *p < 0.05, **p < 0.01, ***p < 0.001.

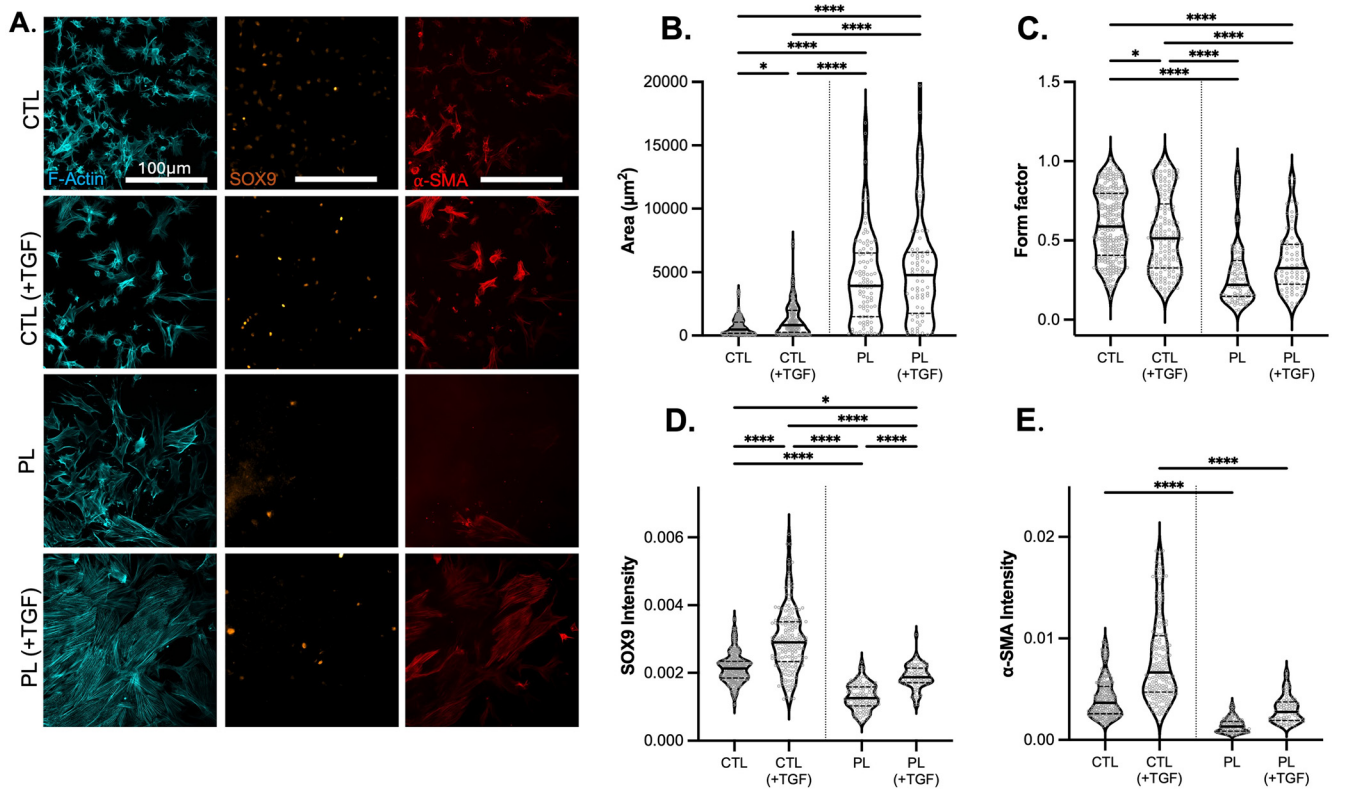

Fig. 4 [A] Staining for F-actin, SOX9, and α-SMA for MDCs cultured for 3 days in fibrin gels without or with platelet lysate (in gel), without or with TGF-β3 (in media). Scale bar = 100 μm. Quantification of [B] cell area, [C] form factor, [D] Sox-9 intensity, and [E] α-SMA intensity on a per cell basis. $n > 50$ cells per group. *$p < 0.05$, ****$p < 0.0001$.

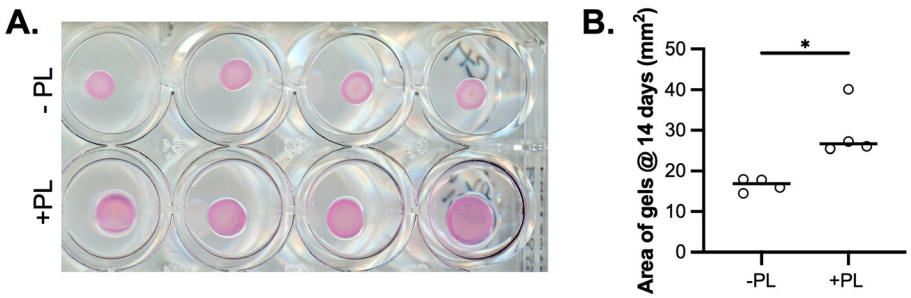

Fig. 5 [A] Images of fibrin gels without or with PL, after 2 week culture. [B] Area of gels at 14 days for quantification of contraction. $n = 4$ per group. *$p < 0.05$.

contraction suggests that PL influences fibrin network stability, potentially supporting long-term volumetric retention. While contraction was variable across this donor and additional donors, PL incorporation consistently led to a greater average area (Fig. S3).

In vivo pig study

Biomechanical testing. Biomechanical testing (Fig. 6A and B) revealed considerable variability, even at different positions within the same defect. For this reason, values are presented separately for each animal. Both instantaneous (Fig. 6C) and equilibrium (Fig. 6D) moduli were mostly comparable between the groups, with a few individual comparisons barely showing statistical significance ($0.01 < p < 0.05$). Overall, all groups were considerably lower than healthy tissue, suggesting that PL supplementation does not enhance repair tissue stiffness.

Macroscopic observations and micro-CT analysis

Macroscopic observations of defects demonstrated that all groups were red and highly vascularized (Fig. 7A – top). Furthermore, all defects were recessed below the neighboring cartilage surfaces. Of note was that distal defects showed quite variable geometry due to proximity to the notch, making μCT analyses difficult. For that reason, these defects were removed

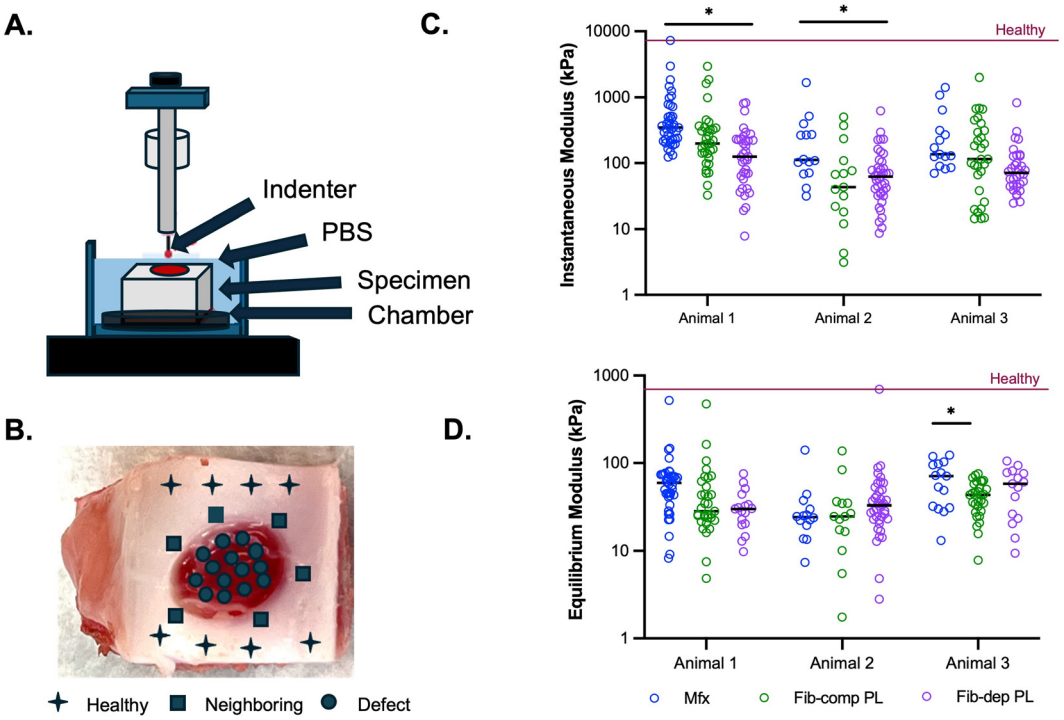

Fig. 6 [A] Schematic of Biomomentum Mach-1 indentation testing. [B] Representative image of positions on cartilage defect that were tested. [C] Instantaneous modulus and [D] equilibrium modulus of each group, broken down by animal. Red line indicates healthy tissue. *$p < 0.05$.

from analysis, leaving $n = 4$ per group. μCT imaging (Fig. 7A – bottom) revealed that Mfx defects experienced significant contraction. The degree of defect fill in these images (Fig. 7B) was quantified, validating that PL-treated Mfx defects (both Fib-comp and Fib-dep) experienced less average contraction compared to Mfx controls, albeit not statistically significant. μCT quantification of subchondral bone changes (outlined by a white dashed line, Fig. 7A) revealed no statistical changes between groups (Fig. 7C), though the Fib-comp group showed values closes to healthy tissue.

Histology and ICRS II scoring

Safranin O/Fast Green staining (Fig. 8A) showed that all three repair tissue groups did not exhibit repair tissue, on average, that resembled native healthy cartilage. Defects in all three groups were clearly recessed and mostly void of red proteoglycan staining. A couple defects across all three groups exhibited deeper proteoglycan staining and areas of rounded cells (SI Fig. S1), but this finding was not consistent. The corresponding ICRS II scoring showed no significant differences in tissue architecture or histological quality between the PL-treated and control groups (Fig. 8B).

Discussion

This study aimed to evaluate platelet lysate (PL) as a potential augmentation strategy for microfracture-based cartilage repair by assessing its effects on cell activity, fibrin gel properties, and tissue contraction within the defect site. Different PL formulations were evaluated to isolate the role of fibrinogen and assess whether PL alone could augment microfracture for improved tissue repair, or if the added fibrinogen was the key contributor to this effect. However, no significant differences were observed between the PL groups. Our findings did demonstrate that PL supplementation enhanced cell proliferation, modified fibrin gel microstructure, and improved resistance to contraction, suggesting its potential to support early tissue repair. However, PL did not appear to improve *in vitro* chondrogenesis or *in vivo* repair tissue quality, calming its excitement as an adjuvant to Mfx. Across three independent human donors, consistent trends were observed in clot contraction (macrogels) as well as in proliferation, SOX9, α-SMA, and morphology (microgels), with no evidence of donor-dependent variability (see the SI).

In a two-dimensional culture, PL supplementation enhanced MDC proliferation, as indicated by increased Ki-67 staining, while maintaining metabolic activity without inducing stress, supporting its potential as a serum alternative.[27,33,34] The observed structural and mechanical modifications in fibrin gels upon PL incorporation suggest that PL actively influences fibrin self-assembly.[35] The presence of distinct "flower-like" microstructures and the increased fibril diameter, as confirmed by SEM, indicate that PL components like thrombin and fibrinogen may alter fibrin polymerization dynamics.[36,37] Additionally, the increased gel

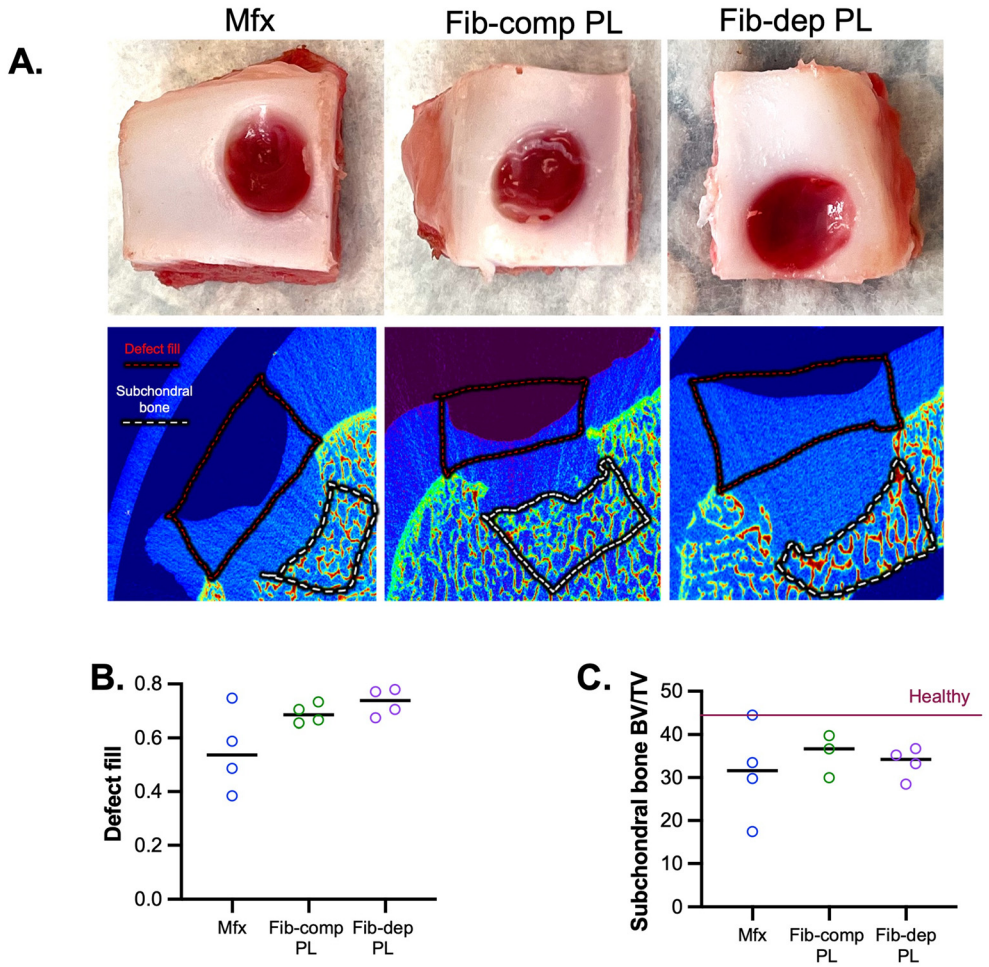

Fig. 7 [A] Macroscopic view and micro-CT images of pig cartilage defects. Red dash line approximates box used to measure defect fill, and the white dash line indicates region of subchondral bone that was analyzed. [B] Defect fill. [C] Subchondral bone BV/TV. *n* = 4 per group.

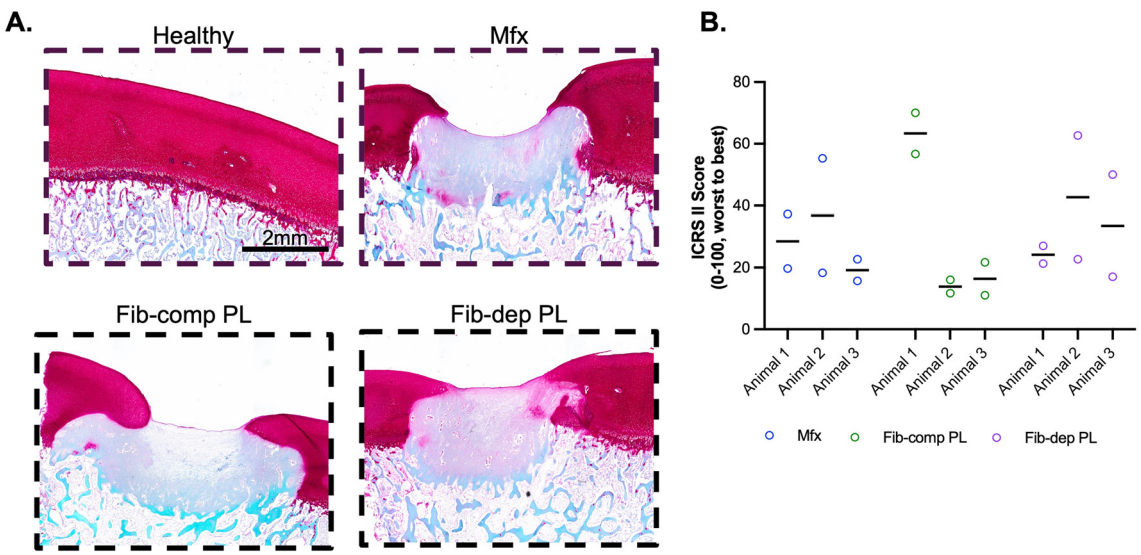

Fig. 8 [A] Representative Safranin O-Fast Green images of pig cartilage defects. Scale bar = 2 mm. [B] ICRS II scores of pig cartilage defects, broken down by animal. *n* = 2 defects per animal per group.

stiffness observed in mechanical testing suggests that PL-mediated alterations to the fibrin network could enhance structural integrity, potentially influencing cell migration and differentiation.[38] In parallel, cells within PL-containing gels displayed a denser distribution, suggesting improved proliferation, as further supported by increased proliferation markers such as Ki-67.[36] Additionally, the increase in cell area and rounder morphology in PL gels suggests a shift in cytoskeletal organization, potentially influencing differentiation pathways and suggesting greater cell "activity".[39,40] However, Sox-9 and α-SMA expression were both decreased in PL-containing gels, indicating a reduction in both chondrogenic and fibrotic activity compared to controls. This suggests that while PL enhances proliferation and alters cell morphology, it may also modulate differentiation cues within the fibrin gel environment.[41] PL-supplemented gels also exhibited a larger area after two weeks of culture, indicating superior resistance to contraction and potential for better defect filling and volumetric maintenance after Mfx.[42,43]

In the *in vivo* pig model, all groups received microfracture; the control group received no additional augmentation. Mechanical testing revealed no significant differences in stiffness between PL-treated and control groups, indicating that PL supplementation did not substantially alter the mechanical properties of the regenerated tissue at this early time point. We chose a 5 week timepoint to capture early clot remodeling and stabilization, recognizing that longer-term studies are needed to evaluate whether these early effects translate into durable cartilage regeneration. This aligns with previous studies showing that early-stage cartilage repair is often dominated by structural remodeling rather than immediate mechanical improvements.[44] While we have shown that PL enhanced fibrin architecture and reduce gel contraction *in vitro*, these modifications did not translate into measurable differences in tissue mechanics, highlighting the challenge of achieving native-like mechanical properties in early repair.

Beyond mechanical properties, μCT analysis provided further insight into tissue regeneration and defect healing. No significant differences were observed in subchondral bone parameters among the treatment groups, suggesting that, at this time point, neither the presence nor composition of PL-based treatments markedly influenced subchondral bone remodeling or integrity. However, quantification of defect fill showed slightly improved outcomes in the fibrin competent (Fib-Comp PL) and fibrin depleted (Fib-Dep PL) groups, which may indicate that localized PL delivery strategies enhance early defect stabilization.[42,43] Histological analysis further corroborated these findings, as ICRS II scoring revealed no significant differences in cartilage repair quality between treatment groups. These results suggest that while PL-based strategies may enhance initial defect stabilization, longer-term studies are needed to assess whether these early benefits translate into sustained cartilage repair.

Altogether, these results suggest that while PL may contribute to early-stage cell proliferation and activity, these benefits may not yet translate into measurable improvements in tissue composition or organization at this stage of healing. While the *in vitro* studies included three independent donors, larger cohorts will be needed to fully account for inter-individual variability. Notably, an important limitation of this *in vivo* model is that the defects were osteochondral and thus more invasive to the subchondral bone than standard microfracture procedures. Removing subchondral bone may have compromised the natural underlying scaffolding essential for cartilage regeneration, potentially contributing to suboptimal repair tissue.[45–47] Additionally, the placement of multiple defects in close proximity may have influenced both local tissue healing and the mechanical environment.[48,49] A more standard microfracture approach (with minimal disruption to the subchondral bone) and better spatial separation of defects could yield more definitive insight into PL's capacity to enhance cartilage regeneration. Moreover, extended evaluations of mechanical properties over longer time frames (3, 6 month), along with molecular and biochemical assessments of chondrogenic *versus* fibrotic pathways, may help refine PL-based strategies. Future directions may also include combining PL with emerging regenerative strategies to further enhance repair.[50] Finally, considerable animal variability was observed, motivating the need to perform additional studies for improved scientific rigor and statistical power.[51] This study was limited by a small cohort (n = 3 animals), and results should be interpreted as exploratory and hypothesis-generating. Overall, these early results underline the promise of PL in facilitating cell proliferation and reducing defect contraction but also underscore the importance of optimizing both PL composition and surgical technique to achieve structurally and functionally cartilage repair.

Conclusion

This study demonstrated that incorporating platelet lysate (PL) into fibrin-based constructs may support cell activity and help maintain defect volume in both *in vitro* and *in vivo* models. However, PL supplementation did not markedly influence subchondral bone remodeling or functional mechanical properties of repair tissue. Histological analysis further corroborated these findings, suggesting that while PL may contribute to cell proliferation, these benefits did not provide measurable improvements in tissue composition. This study was limited by sample size, with four pigs included in the analysis. While this number is modest, it reflects the inherent logistical and ethical constraints of large animal studies. Importantly, the observed outcomes were consistent across animals, supporting the reproducibility of the findings. To our knowledge, this is the first large animal study directly evaluating PL as an adjunct to microfracture. While early outcomes were modest, this model provides a critical foundation for refining PL-based approaches. Future work will battle limitations related to the model and evaluation of PL components most influential in healing. These results highlight that while PL can provide some enhancement, it requires additional testing before clinical adoption to augment Mfx.

Conflicts of interest

J. M. P. is a co-founder and owns equity in Forsagen LLC. This involvement did not influence this study.

Data availability

Due to the large file sizes of confocal and other imaging datasets, the raw data is stored on our local institutional server, however we are happy to share as needed.

Supplementary information (SI) is available. See DOI: https://doi.org/10.1039/d5bm00372e.

Acknowledgements

This work was supported by the Regenerative Engineering and Medicine (REM) Center, which is supported by the National Center for Advancing Translational Sciences of the National Institutes of Health under Award Number UL1TR002378. The content is solely the responsibility of the authors and does not necessarily represent the official views of the National Institutes of Health. We also thank the Emory Department of Orthopaedics and the Musculoskeletal Research Center, as well as the Department of Veterans Affairs, for their support.

References

1 M. Wang, Y. Wu, G. Li, Q. Lin, W. Zhang, H. Liu and J. Su, *Mater. Today Bio.*, 2024, **24**, 100948.
2 A. J. Sophia Fox, A. Bedi and S. A. Rodeo, *Sports Health*, 2009, **1**, 461–468.
3 A. H. Gomoll and T. Minas, *Wound Repair Regen.*, 2014, **22**, 30–38.
4 A. Litwic, M. Edwards, E. Dennison and C. Cooper, *Br. Med. Bull.*, 2013, **105**, 185–199.
5 C. Erggelet and P. Vavken, *J. Clin. Orthop. Trauma*, 2016, **7**, 145–152.
6 M. Hasson, L. M. Fernandes, H. Solomon, T. Pepper, N. L. Huffman, S. A. Pucha, J. T. Bariteau, J. M. Kaiser and J. M. Patel, *Cells Tissues Organs*, 2024, **213**(6), 523–537.
7 H. M. Zlotnick, R. C. Locke, B. D. Stoeckl, J. M. Patel, S. Gupta, K. D. Browne, J. Koh, J. L. Carey and R. L. Mauck, *Eur. Cells Mater.*, 2021, **41**, 546–557.
8 A. C. DiBartola, J. S. Everhart, R. A. Magnussen, J. L. Carey, R. H. Brophy, L. C. Schmitt and D. C. Flanigan, *Knee*, 2016, **23**, 344–349.
9 J. L. Carey, *J. Bone Joint Surg. Am.*, 2012, **94**, e80.
10 K. Mithoefer, T. McAdams, R. J. Williams, P. C. Kreuz and B. R. Mandelbaum, *Am. J. Sports Med.*, 2009, **37**, 2053–2063.
11 J. M. Patel, K. S. Saleh, J. A. Burdick and R. L. Mauck, *Acta Biomater.*, 2019, **93**, 222–238.
12 L. A. Fortier, J. U. Barker, E. J. Strauss, T. M. McCarrel and B. J. Cole, *Clin. Orthop.*, 2011, **469**, 2706–2715.
13 C. Wen, L. Xu, X. Xu, D. Wang, Y. Liang and L. Duan, *Arthritis Res. Ther.*, 2021, **23**, 277.
14 M. Wu, S. Wu, W. Chen and Y.-P. Li, *Cell Res.*, 2024, **34**, 101–123.
15 L. Sun, M. R. Reagan and D. L. Kaplan, *Orthop. Res. Rev.*, 2010, **2010**, 85–94.
16 W. Wang, D. Rigueur and K. M. Lyons, *Birth Defects Res. C Embryo Today*, 2014, **102**, 37–51.
17 P. Everts, K. Onishi, P. Jayaram, J. F. Lana and K. Mautner, *Int. J. Mol. Sci.*, 2020, **21**, 7794.
18 G. Filardo, E. Kon, R. Buda, A. Timoncini, A. Di Martino, A. Cenacchi, P. M. Fornasari, S. Giannini and M. Marcacci, *Knee Surg. Sports Traumatol. Arthrosc.*, 2011, **19**, 528–535.
19 T. E. Foster, B. L. Puskas, B. R. Mandelbaum, M. B. Gerhardt and S. A. Rodeo, *Am. J. Sports Med.*, 2009, **37**, 2259–2272.
20 Y. Liang, J. Li, Y. Wang, J. He, L. Chen, J. Chu and H. Wu, *Cartilage*, 2022, **13**, 19476035221118419.
21 J. Fitzpatrick, M. K. Bulsara, P. R. McCrory, M. D. Richardson and M. H. Zheng, *Orthop. J. Sports Med.*, 2017, **5**, 2325967116675272.
22 K. Mautner, G. A. Malanga, J. Smith, B. Shiple, V. Ibrahim, S. Sampson and J. E. Bowen, *PM R*, 2015, **7**, S53–S59.
23 L. da Fonseca, G. S. Santos, S. C. Huber, T. M. Setti, T. Setti and J. F. Lana, *J. Clin. Orthop. Trauma*, 2021, **21**, 101534.
24 T. Burnouf, H. A. Goubran, T.-M. Chen, K.-L. Ou, M. El-Ekiaby and M. Radosevic, *Blood Rev.*, 2013, **27**, 77–89.
25 G. Strandberg, F. Sellberg, P. Sommar, M. Ronaghi, N. Lubenow, F. Knutson and D. Berglund, *Transfusion*, 2017, **57**, 1058–1065.
26 L. da Fonseca, G. S. Santos, S. C. Huber, T. M. Setti, T. Setti and J. F. Lana, *J. Clin. Orthop. Trauma*, 2021, **21**, 101534.
27 V. Becherucci, L. Piccini, S. Casamassima, S. Bisin, V. Gori, F. Gentile, R. Ceccantini, E. De Rienzo, B. Bindi, P. Pavan, V. Cunial, E. Allegro, S. Ermini, F. Brugnolo, G. Astori and F. Bambi, *Stem Cell Res. Ther.*, 2018, **9**, 124.
28 G. Hassan, M. Bahjat, I. Kasem, C. Soukkarieh and M. Aljamali, *Cell. Mol. Biol. Lett.*, 2018, **23**, 11.
29 M. Guiotto, W. Raffoul, A. M. Hart, M. O. Riehle and P. G. di Summa, *J. Transl. Med.*, 2020, **18**, 351.
30 T. Burnouf, M.-L. Chou, D. J. Lundy, E.-Y. Chuang, C.-L. Tseng and H. Goubran, *J. Biomed. Sci.*, 2023, **30**, 79.
31 L. da Fonseca, G. S. Santos, S. C. Huber, T. M. Setti, T. Setti and J. F. Lana, *J. Clin. Orthop. Trauma*, 2021, **21**, 101534.
32 B. C. Halpern, S. Chaudhury and S. A. Rodeo, *HSS J.*, 2012, **8**, 137–145.
33 L. Tolosa, A. Bonora-Centelles, M. T. Donato, V. Mirabet, E. Pareja, A. Negro, S. López, J. V. Castell and M. J. Gómez-Lechón, *Transplantation*, 2011, **91**, 1340–1346.
34 S. Palombella, C. Perucca Orfei, G. Castellini, S. Gianola, S. Lopa, M. Mastrogiacomo, M. Moretti and L. de Girolamo, *Stem Cell Res. Ther.*, 2022, **13**, 142.
35 T. M. Fortunato, C. Beltrami, C. Emanueli, P. A. De Bank and G. Pula, *Sci. Rep.*, 2016, **6**, 25326.

36 T. Canceill, G. Jourdan, P. Kémoun, C. Guissard, Y. A. Monsef, M. Bourdens, B. Chaput, S. Cavalie, L. Casteilla, V. Planat-Bénard, P. Monsarrat and I. Raymond-Letron, *Int. J. Mol. Sci.*, 2023, **24**, 2206.
37 A. A. Solbu, D. Caballero, S. Damigos, S. C. Kundu, R. L. Reis, Ø. Halaas, A. S. Chahal and B. L. Strand, *Mater. Today Bio*, 2022, **18**, 100537.
38 T. Luo, B. Tan, L. Zhu, Y. Wang and J. Liao, *Front. Bioeng. Biotechnol.*, 2022, **10**, DOI: 10.3389/fbioe.2022.817391.
39 J. P. Rodríguez, M. González, S. Ríos and V. Cambiazo, *J. Cell. Biochem.*, 2004, **93**, 721–731.
40 C. Radermacher, A. Rohde, V. Kucikas, E. M. Buhl, S. Wein, D. Jonigk, W. Jahnen-Dechent and S. Neuss, *Gels*, 2024, **10**, 820.
41 S. M. C. Bruekers, M. Jaspers, J. M. A. Hendriks, N. A. Kurniawan, G. H. Koenderink, P. H. J. Kouwer, A. E. Rowan and W. T. S. Huck, *Cell Adhes. Migr.*, 2016, **10**, 495–504.
42 X. Xie, C. Zhang and R. S. Tuan, *Arthritis Res. Ther.*, 2014, **16**, 204.
43 Q. Zhang, H. Zhou, D. Li, Y. Zhong, Y.-F. Zhao, J. Yan and H. Zhao, *J. Orthop. Surg.*, 2024, **19**, 669.
44 H. Alizadeh Sardroud, T. Wanlin, X. Chen and B. F. Eames, *Front. Bioeng. Biotechnol.*, 2022, **9**, 787538.
45 A. H. Gomoll, H. Madry, G. Knutsen, N. van Dijk, R. Seil, M. Brittberg and E. Kon, *Knee Surg. Sports Traumatol. Arthrosc.*, 2010, **18**, 434–447.
46 K. Higa, N. Kitamura, K. Goto, T. Kurokawa, J. P. Gong, F. Kanaya and K. Yasuda, *BMC Musculoskelet. Disord.*, 2017, **18**, 210.
47 B. J. Ahern, J. Parvizi, R. Boston and T. P. Schaer, *Osteoarthritis Cartilage*, 2009, **17**, 705–713.
48 J. R. Steadman, W. G. Rodkey, S. B. Singleton and K. K. Briggs, *Oper. Tech. Orthop.*, 1997, **7**, 300–304.
49 B. J. Erickson and A. Gomoll, in *Complications in Orthopaedics: Sports Medicine*, ed. S. R. Thompson and M. R. Schmitz, Elsevier, Philadelphia, 2019, pp. 168–175.
50 C. Gao, Y. Chen, X. Wen, R. Han, Y. Qin, S. Li, R. Tang, W. Zhou, J. Zhao, J. Sun, Z. Li, Z. Tan, D. Wang and C. Zhou, *J. Mater. Chem. B*, 2025, **13**, 2254–2271.
51 J. M. Patel, M. L. Sennett, A. R. Martin, K. S. Saleh, M. R. Eby, B. S. Ashley, L. M. Miller, G. R. Dodge, J. A. Burdick, J. L. Carey and R. L. Mauck, *Cartilage*, 2021, **13**, 1676S–1687S.